Design, Synthesis, and Testing of a Novel 3,5-Dimethoxycinnamic Acid-Based Cathepsin C Inhibitor for the Treatment of Inflammatory Bowel Disease

Fillip Fuňák

The North Carolina School of Science and Mathematics

1219 Broad St, Durham, NC, 27705

Mentor: Dr. Timothy Anglin

Abstract

Inflammatory bowel disease (IBD), which encompasses Crohn's disease and ulcerative colitis, affects about 5 million people worldwide and is caused by the inflammation of the gastrointestinal tract. Current treatments including surgery, anti-inflammatory medications, and cytokine inhibitors, often fall short because of their limited efficacy, side effects, or narrow cytokine targeting. To address this need, this project focused on developing a novel small-molecule inhibitor for Cathepsin C (CTSC), a cysteine protease that activates serine proteases. Serine proteases are responsible for activating multiple pro-inflammatory cytokines, which induce inflammation and further elevate IBD. 3,5-dimethoxycinnamic acid was chosen as the starting scaffold, ~~since this compound is known for having anti-inflammatory and antioxidant properties, was affordable, and had an ideal structure for the intended modifications.~~ Through computational modeling in Schrödinger Maestro, over 200 different variants of 3,5-dimethoxycinnamic acid were docked to the CTSC protein and screened for docking scores and ADME pharmacokinetic properties. Structure 228 (S228) was selected as the ideal candidate, was synthesized, and evaluated in *Drosophila melanogaster* via the SMURF assay, which was given DSS-induced IBD to test S228's efficacy in vivo. S228 demonstrated measurable improvements in gut integrity and survival. These results suggest that upstream inhibition of CTSC may offer a new therapeutic strategy for IBD by significantly reducing cytokine driven inflammation.

1 Inflammatory Bowel Disease Introduction

1.1 Background

Inflammatory Bowel Disease (IBD) affects about 5 million people worldwide, with cases rising each year. Today, more than 1% of adults living in the U.S. are diagnosed with IBD at some point in their lives [1]. IBD is characterized by the inflammation of the gastrointestinal tract (GI tract), due to the overproduction and release of inflammatory cytokines that bind to receptors in the intestines, inducing inflammation. There are 2 main types of IBD: Crohn's disease (CD), which can affect any part of the GI tract, from the mouth to the anus, and every layer of the wall lining; and ulcerative colitis (UC), which causes inflamed sores (ulcers) and is limited to the colon and rectum, affecting only the innermost colon lining [2]. Both conditions cause severe abdominal pain, diarrhea, rectal bleeding, nausea, weight loss, and constipation, significantly reducing a patient's quality of life. IBD is influenced by numerous environmental and genetic factors. For example, individuals with certain gene variants have weakened epithelial barriers, allowing bacteria from the colon to enter the underlying tissue, triggering an aggressive inflammatory response and inflammation [3]. The immune response in IBD is heavily driven by activated neutrophils, macrophages, and T-cells, all of which release pro-inflammatory cytokines including IL-1β, IL-6, TNF-α, IL-12, and IFN-ɣ [1]. These chemical mediators cause a cycle of epithelial barrier damage and recruit more immune cells, leading to an uncontrolled and chronic immune response. There are currently no cures for IBD, with treatments aiming to reduce inflammation and produce remission [4].

1.2 Current Treatments and Previous Research Conducted

Current treatments include anti-inflammatory medications, surgery to remove a part or the entirety of the colon or rectum, biologics to neutralize inflammation-causing proteins, immunomodulators and corticosteroids to suppress the immune response and release of anti-inflammatory chemicals, and small molecule inhibitors that target cytokines and inflammatory mediators [4]. Although these approaches can alleviate symptoms and inflammation, they are limited by inconsistent efficacy, systemic side effects, and the development of resistance. Recent therapies have shifted towards small-molecule inhibitors that target signaling pathways more precisely. Among these recent therapies, Janus kinase (JAK) inhibitors can target enzymes in the immune system involved in inflammation and have shown clinical promise. Tofacitinib, commonly known as Xeljanz, is among these promising JAK inhibitors and has been approved for IBD treatment [5]. However, the US Federal Food and Drug Administration recently started warning about using tofacitinib, reporting that studies show the drug can lead to an increased risk of heart-related conditions and cancer [4]. Another limitation of many current inhibitors is the narrow targeting of single cytokine pathways. Many popular treatments fall under this category, such as, Skyrizi, risankizumab-rzaa, which targets IL-23; Omvoh, mirikizumab-mrkz, which also targets IL-23; Remicade,

infliximab, which targets TNF-α; and Actemra, tocilizumab, which targets IL-6. However, research shows that targeting a single cytokine pathway has not achieved a widespread reduction in inflammation, making it an ineffective approach. IBD involves a complex system of inflammatory signals, meaning that only stopping one pathway leaves other inflammatory pathways that can take its place. As a result, many patients experience relapses or only have partial responses [6]. Because patients display diverse cytokine profiles, have varying immune responses to IBD, and because IBD has a heterogeneous etiology, the key cytokine driving gut inflammation can vary from patient to patient. Without integrating patient specific features, single cytokine therapies may cause inconsistent results [7, 8]. By targeting upstream pathways that regulate multiple cytokines, the likelihood of suppressing the key inflammatory driver in a given patient increases.

1.3 Small Molecule Pharmaceuticals

Small molecule inhibitors are characterized by their small size/molecular weight, which increases oral bioavailability, allowing for efficient systemic delivery. Unlike large biologics such as monoclonal antibodies, small molecules can be administered orally rather than by injection, improving patient satisfaction and significantly reducing treatment costs [9]. Their small size also enables them to cross cell membranes, penetrate tissues more easily, and are effective at targeting intracellular pathways [8]. Furthermore, small molecule inhibitors are generally less expensive to produce and easier to formulate into different dosage forms [8, 9]. These advantages make small molecule pharmaceuticals an attractive therapeutic target for chronic diseases, such as IBD, where convenient, cost effective, and long lasting treatments are desired.

1.4 Cathepsin C Background

Emerging research suggests that Cathepsin C (CTSC), also known as dipeptidyl peptidase I, plays a central role in regulating neutrophil activity and inflammatory signaling, making it an ideal therapeutic target for IBD. CTSC is a lysosomal cysteine protease expressed in immune cells including neutrophils, mast cells, and cytotoxic lymphocytes [10, 11, 12]. Unlike many proteases that act independently, CTSC forms a tetramer, meaning it is built from four identical subunits that expose active sites used for protein processing [11, 12]. The main job of CTSC is to act as a main activator for a broad range of serine proteases. CTSC works by removing a dipeptide from the N-terminus of inactive serine protease zymogens, with the main ones being granzymes A and B, proteinase 3 (PR3), cathepsin G (CatG), neutrophil elastase (NE), NSP-4, tryptase, and mast cell chymase prompting their conversion into active forms [12]. Once activated, these proteases drive immune defense, tissue remodeling, and importantly, cytokine release. In IBD, CTSC becomes a key driver of mucosal damage. Activated neutrophil serine

proteases (NSP's) accumulate in the intestinal mucosa and subsequently break down the epithelial barrier [12]. In particular, CTSC-regulated proteases trigger the release of multiple pro-inflammatory cytokines—including IL-1β, IL-6, TNF-α, CCL3, CXCL2, GM-CSF, and many others—both directly, by stimulating immune cells, and indirectly, through the chemokine mediated recruitment of additional neutrophils, cytotoxic T-cells, mast cells, natural killer T-cells, and monocytes [11, 12]. This then leads to a cascade of inflammation, and the recruitment of more immune cells, further increasing cytokine production, and continuing tissue damage, as shown in **figure 1**. This can even lead to NETosis, where neutrophils release webs of DNA and enzymes to trap pathogens, damaging tissues in the process, further inducing IBD [11]. While this system is essential and beneficial for normal immunity, its overactivation in the gut can cause significant epithelial injury, barrier breakdown, and chronic inflammation. It is important to note that CTSC levels are elevated in IBD patients [13]. Gene knockout testing and inhibition studies have confirmed that inhibiting CTSC is safe [14]. By inhibiting CTSC, the goal is to stop the downstream activation of serine proteases and subsequent cytokine release by CTSC-regulated proteases to reduce IBD inflammation, which would also allow the intestines to heal. Since CTSC sits at such an important intersection in the IBD inflammatory cascade, it is a compelling target for therapies that aim to reduce cytokine mediated gut inflammation.

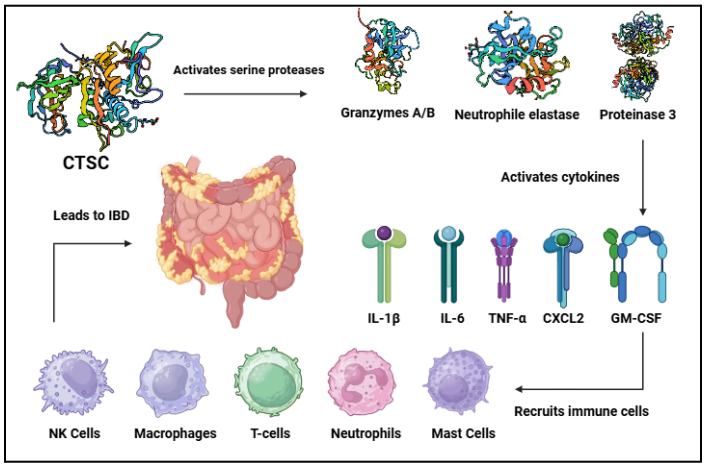

Figure 1: Diagram of the CSTC activation pathway that leads to IBD | Figure made by author using Biorender

1.5 3,5-Dimethoxycinnamic Acid as a Scaffold for Inhibitor Design

3,5-Dimethoxycinnamic acid is a cinnamic acid derivative with two methoxy groups at the 3 and 5 positions on a benzene ring and an α,β-unsaturated carboxylic acid chain, as shown in **figure 2**. 3,5-dimethoxycinnamic acid was selected because the carboxylic acid group provides a functional place for further modifications and adds flexibility to help the ligand fit better into the binding pocket of CTCS. Its structure is already known for antioxidant and anti-inflammatory properties, which are sought after in IBD treatment, especially in a disorder where oxidative stress and inflammation work together to cause

intestinal tissue damage [15, 16]. Studies have also shown that methoxylated cinnamic acids can neutralize unstable free radicals and reduce lipid peroxidation, which could disrupt cell function and further lead to inflammation [17].

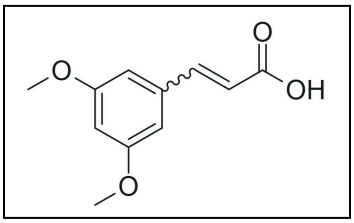

Figure 2: Structure of 3,5-dimethoxycinnamic acid which was used as the starting compound for S228 | Figure made by author using MarvinSketch

2 Scientific Aim

The goal of this project was to design, synthesize, and test a novel derivative of 3,5-dimethoxycinnamic acid as a potential inhibitor of CTSC aimed to treat IBD. Using scaffold-based ligand design, computational docking, and ADME property predictions, a candidate was identified and optimized. A synthesis was developed for feasibility, and the small molecule inhibitor was then synthesized and tested in *Drosophila melanogaster* to test the inhibitor's performance in vivo.

3 Methodology

3.1 Computational Design

Protein Preparation: Computational design was done in the Schrödinger Maestro Suite. The Cathepsin C protein complex (PDB 4CDE) was prepared using Protein Preparation Workflow. To prepare the protein, extra waters were removed, side chains were filled in, and a structural minimization was performed. 4CDE was selected due to its good ligand structure quality compared to other CTSC proteins in the Protein Data Bank. The CTSC binding pocket was located using the Glid Grid feature and with the help of the cognate ligand present in the PDB file. Important residues for CTSC inhibition were found using previous research [14].

Ligand Preparation: Ligands were prepared using the LigPrep feature in the Schrödinger Maestro Suite. To prepare the ligands, missing hydrogens were added, geometries were optimized, and different protonation states and stereoisomers were tested. A preparation pH of 6.5±1.0 was used for all ligands to approximate the physiological environment of the duodenum, the first portion of the small intestines, where IBD most commonly occurs. This pH range was selected to ensure the designed ligand would remain active and effective by the time it reached the therapeutic region. In addition, the condition aligns

with future plans toward targeted biodelivery strategies, providing a framework for subsequent optimization.

Docking Score: The docking score was one of the metrics used to determine a drug candidate. It provides a computational estimate of the strength of the interaction between the CTSC binding pocket and the ligand, with a more negative number showing a higher likelihood of binding to the target binding site within the binding pocket. Before docking, the LigPrep tool was used to expand possible ionization states, enumerate stereoisomers, and generate low energy 3D structures for the ligands that would be docked to the CTSC protein. The glide feature was then used to dock all ligands to the CTSC protein. **Figure 3** shows CatC inhibitor 10 docked in the binding pocket of the CSTC protein [14]. This docking score was saved as a baseline measurement for subsequent docking.

Figure 3: CatC inhibitor 10 (white) in the binding pocket of the CTSC protein | Figure made by author using Schrödinger Maestro

Scaffold based Ligand Design: Previous docking studies have identified CYS-234, ASP-1, ASN-380, and HIE-381 as important activation residues for CTSC inhibition, with CYS-234 being the critical and decisive determinant of inhibitory potential [13, 14]. Initially, a library of structural variants were docked and analyzed. 3,5-dimethoxycinnamic acid, shown in **figure 2**, was ultimately chosen as the baseline scaffold due to its improved synthetic accessibility and more practical suitability for the intended modifications. The chosen baseline scaffold preserved the essential structural features necessary for activation while enabling a more convenient and cost effective route for further ligand development. A total of 200 ligands were designed by hand using the baseline scaffold, and the best docking ligands were selected for the next phase of pharmacokinetic selection.

ADME Pharmacokinetic Properties: Compounds that had the highest docking scores were selected for pharmacokinetic, cytotoxicity, and Lipinski rule violation screening. Ligands with 2 or more Lipinski

violations were not considered. Additional ADME properties included: QPlogHERG, predicted inhibition of HERG K+ channels, an important cardiotoxicity risk; QPlogS, predicted aqueous solubility, important for oral bioavailability; QPlogKhsa, predicted binding affinity to human serum albumin, which affects the amount of free drug available in the bloodstream; and CNS, estimated blood-brain barrier penetration of the drug. Acceptable ranges for the following ADME properties were selected based on the QikProp manual: a QPlogHERG score above -6 (with the CatC inhibitor 10 having a score of -6.512), a QPlogS score above -2, a QPlogKhsa score within the -1.5 and 1.5 range, a CNS score of -2, and less then 2 Lipinski rule violations [18].

3.2 Synthesis of Ligand S228

Step 1 Synthesis: Synthesis of S228 followed a 3-step process. The first synthesis step involved the nitration of the dimethoxybenzene ring, as shown in **figure 4**. 2.004g, 9.6 mmol, of the baseline scaffold 3,5-dimethoxycinnamic acid (Sigma Aldrich) was diluted in as little acetonitrile (Sigma Aldrich) as possible in a separate beaker. Into a 50 mL round-bottom flask set over an ice bath and stir bar, 0.533 mL of conc. H_2SO_4 (Fisher Scientific) and 0.608 mL of conc. HNO_3 (Fisher Scientific) was added. While stirring, the diluted 3,5-dimethoxycinnamic acid was added dropwise over 2 minutes into the round bottom flask. This was allowed to stir for 5 minutes, constantly over the ice bath. This mixture was then added to a 100 mL beaker filled with 50 mL of ice cold deionized H_2O and stirred to allow the nitrated solvent to precipitate out. After letting this sit for 3 minutes, the solids were vacuum filtered through a filter paper that weighed 0.255 g, and then washed with deionized H_2O. The nitrated precipitate was then diluted in a 25 mL beaker filled with 5 mL of hot ethanol (Fisher Scientific) and immediately put into an ice bath to recrystallize for 20 minutes, as shown in **figure 5**. The recrystallized solids were then vacuum filtered once again, through a 0.231 g filter paper. The filter paper and solids were then transferred to a glass weight plate and placed in the oven to dry at 60 ℃ for 15 minutes. After drying, 4-nitro-3,5-dimethoxycinnamic acid (compound 1) was collected and transferred to a glass vial, as shown in **figure 5**, producing a 31.4% yield [19]. FTIR spectroscopy, using the Shimadzu IRSpirit, was conducted to characterize the formed compound, and 0.610 g of compound 1 remained after testing.

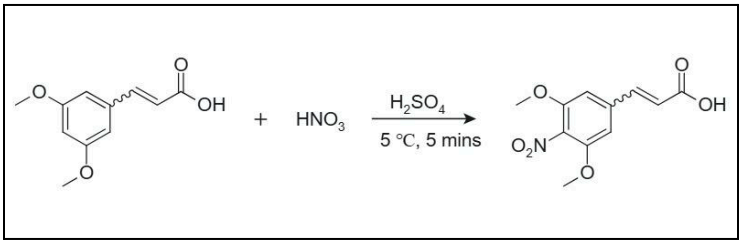

Figure 4: Compound 1 synthesis scheme. Nitration of dimethoxybenzene ring | Figure made by author using MarvinSketch

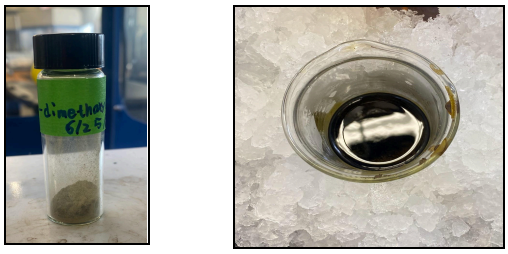

Figure 5: (Left) Compound 1 in glass vial, and (Right) compound 1 precipitate dissolved in hot ethanol | Photo taken by author

Step 2 Synthesis: The second synthesis step involved the conversion of a carboxylic acid to an amide via N,N'-Dicyclohexylcarbodiimide (DCC) coupling, as shown in **figure 6**. This reaction was done in a 1:10 ratio of compound 1 to 1,3-diamino-2-propanol. This ensured that during DCC coupling, unreacted compound 1 would be statistically favored to react with another unreacted compound 1 then with a coupled compound 1, decreasing the chance of dimer formation. 0.307 g, 1.21 mmol, of compound 1 was added into a 30 mL beaker with 2.52 g, 12.2 mmol, of DCC (Sigma Aldrich) and dissolved with as little tetrahydrofuran (THF) as possible. 1.0 g, 11.09 mmol, of 1,3-diamino-2-propanol (Thermo Scientific) was added to a 25 mL round-bottom flask and dissolved with as little THF as possible. The 25 mL round-bottom flask was placed over an ice bath with a stir bar and the compound 1/DCC mixture was added dropwise to the round-bottom flask while stirring over the ice bath until all was added. The mixture was stirred at room temperature for 3 days, as shown in **figure 7**. Reaction progress was checked half way through the reaction using thin layer chromatography (TLC) to ensure the reaction was occurring. After 2 days of mixing, the reaction was filtered through a vacuum filter, taken up with ethyl acetate (Fisher Scientific), and washed with sodium bicarbonate (Fisher Scientific) to produce unpurified compound 2. Subsequent TLC testing was conducted using methanol (Fisher Scientific) as the mobile phase, showing that 3,5-dimethoxycinnamic acid and (E)-N-(2-amino-3-hydroxypropyl)-3-(4-nitro-3,5-dimethoxyphenyl) prop-2-enamide (compound 2) traveled to the solvent front while 1,3-diamino-2-propanol remained at the base line. To further purify the product, column chromatography was performed, with the expectation that 1,3-diamino-2-propanol would stay in the column while the desired compound 2 would exit the column. The crude product was diluted in methanol (Fisher Scientific) and loaded onto the column to drip for 3 days. TLC was conducted once again with methanol as the mobile phase. A drop from each of the 5 vials containing dripped product from column chromatography was tested, as shown in **figure 7**. The contents of vials 1-3, where majority of the compound 2 was found, were added to a 25 mL round-bottom flask and methanol was roto evaporated (rotovap). After rotovap, 0.804 g of compound 2 was collected and placed in a 50 mL beaker, for a crude yield of 262%, due to the impurities and viscous state present in the

compound 2 product [20]. FTIR spectroscopy was conducted to characterize the formed compound, and 0.610 g of compound 1 remained after testing.

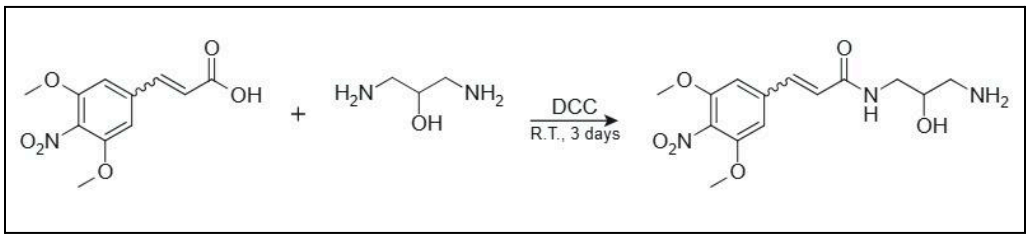

Figure 6: Compound 2 synthesis scheme. Carboxylic acid to amide | Figure made by author using MarvinSketch

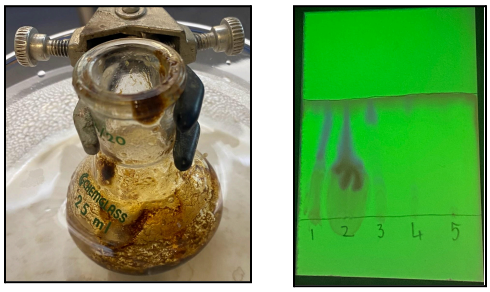

Figure 7: (Left) Compound 2 reaction at room temperature mixed for 3 days, and (Right) TLC plate with samples from 5 column chromatography vials. Vials 1, 2, and 3 had the most visible compound 2 (purple) | Photo taken by author

Step 3 Synthesis: The third synthesis step involved the reduction of an aromatic nitro group into an amine, as shown in **figure 8**. 0.50 g, 1.67 mmol, of compound 2, 0.71 mL of acetic acid (Thermo Scientific), 2.86 mL of ethanol (Fisher Scientific), and 0.286 g of fine Fe powder (Fisher Scientific) were added to a 25 mL round bottom flask. While stirring over an ice bath, 4 drops of conc. HCl was added to the round bottom flask to catalyze the reaction and stirred for 3 minutes. This addition was exothermic. After mixing, the mixture was heated to reflux for 45 minutes. A TLC was taken at time 0 and every 15 minutes after. The mixture was then removed from reflux and allowed to cool to room temperature. The mixture was then filtered by vacuum filter and rotovapped to get a concentrated thick oil. This oil was separated using a separatory funnel with 3.57 mL of ethyl acetate (Sigma Aldrich) and 1.43 mL of deionized H_2O. The product was then basified to a pH of 11 using 6 M NaOH (Fisher Scientific). This basified organic layer was then separated and washed once again with 0.71 ml x 2 sat. aq. $NaHCO_3$ (Fisher Scientific) solution, 0.71 mL x 2 deionized H_2O, 0.71 mL NaCl, and dried with Na_2SO_4 (Sigma Aldrich). This resulting product was then concentrated using rotovap, to give 0.038 g of S228 as a product, for a step 3 yield of 7.6% and an overall yield of 1.52% [21]. An FTIR spectroscopy and an ^{1}H-NMR spectroscopy, using the Nanalysis NMReady 60 Pro, were conducted to verify S228's formation.

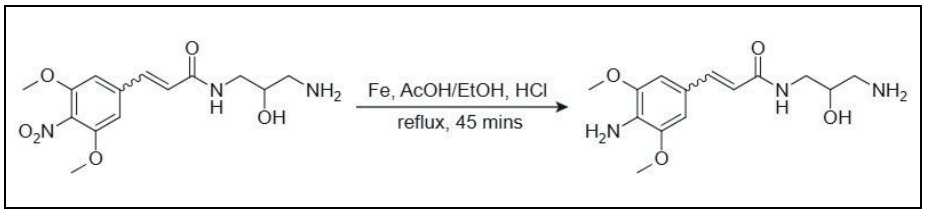

Figure 8: Compound 3 synthesis scheme. Reduction of a nitro group to an amine on the benzene ring | Figure made by author using MarvinSketch

3.3 Biological Testing

Model Organism: *Drosophila melanogaster* was selected as a model organism for the preliminary in vivo screening of anti-inflammatory efficacy. While *Drosophila melanogaster* lacks a direct CTSC ortholog, this model provides a valuable base for initial drug evaluation prior to more resource intensive mammalian studies. The *D. melanogaster* gastrointestinal tract shows conserved responses to inflammatory damage including an increased intestinal permeability and barrier disruption, which are key pathological features of IBD [22]. This model also enables the compounds bioavailability, toxicity, anti-inflammatory activity, and dose-response to be easily accessed. Additionally, due to the translucent nature of the *D. melanogaster* abdomen, direct visualization and characterization of intestinal tissue is possible. This preliminary data is essential for determining whether it is logical to further investigate the compound in mammalian models, where CTSC specific inhibition can be verified.

Drug Dosage Methodology: Following ^{1}H-NMR verification, S228 remained dissolved in DMSO-d_6 at a known concentration. The stock solution concentration was calculated based on the mass of S228 and the volume of DMSO-d_6 used. To prepare working treatment concentrations, dilutions were performed to achieve final concentrations: 0.1 µM, 0.5 µM, 2.5 µM, and 5.0 µM of S228. The required volume of S228/DMSO-d_6 solution was calculated for each target concentration and added directly to fly medium prior to the addition of the *D. melanogaster*. The final DMSO concentration in all treatment groups was calculated to not exceed 0.5% v/v to avoid toxicity.

Experimental Design Overview: *D. melanogaster* testing was split into two groups: one group received S228 before receiving DSS-induced IBD to test S228's potential as a preventative treatment, while the other group received S228 after DSS-induced IBD had developed to test S228's potential as a therapeutic treatment.

SMURF Assay: Figure 9 shows visually how the SMURF assay process works. The preventative group of *D. melanogaster* were maintained in fly medium with different treatment concentrations mixed into

their food for 6 days. The *D. melanogaster* were then transferred to empty vials containing 2% agar for 24 hours to starve. Next, the *D. melanogaster* were transferred to vials containing either a 250 µL of 5% sucrose or a 5% sucrose (Carolina Biological) with 4% DSS (Spectrum Chemicals) solution soaked in a filter paper, to induce IBD for 48 hours. After the 48 hour period, the *D. melanogaster* were transferred to vials containing food with 2.5% w/v Brilliant Blue FCF (Sigma Aldrich) dye to feed for 24 hours [23].

The therapeutic group of *D. melanogaster* was maintained in vials containing either a 250 µL of 5% sucrose or 250 µL of 5% sucrose with 4% DSS solution soaked in a filter paper, to induce IBD for 4 days. The *D. melanogaster* were then transferred to vials containing fly medium with different treatment concentrations mixed into their food to feed for 3 days. After the 3 day period, the *D. melanogaster* were transferred to vials containing food with 2.5% w/v Brilliant Blue FCF dye to feed for 24 hours [23]. The flies were dissected in hemolymph ringer solution (171. 9 mM KCl, 3.0 mM $MgCl_2$, 1.0 mM CaCl2, 25.0 mM NaCl, 10.0 mM HEPES, and 22.5 mM D-glucose adjusted to a pH level of 6.5) and examined under a dissecting microscope [23]. The average blue intestinal intensity was calculated in FIJI ImageJ. The intestinal images were colour deconvoluted under the Brilliant Blue setting, inverted, and a 64x64 pixel box was used as the area of measurement for all trials.

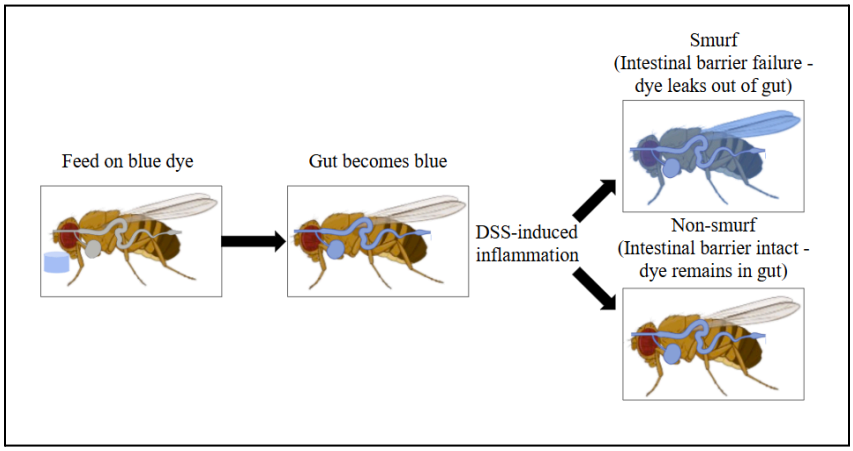

Figure 9: Diagram of SMURF assay process | Figure made by author using Google Slides. Adapted from Livingston et al., 2020 [28]

Survival Assay: Newly hatched D. melanogaster were fed and maintained according to the SMURF assay procedure. Both treatment group types were accessed for 11 days. Time-to-death recordings were recorded for each treatment group once a day. Behavioral change was also accessed twice a day by flipping the glass tubes they were in, and accessing how fast the D. melanogaster climbed back to the top. How fast this occurred was indicative of their health. Flies that took a long time would likely die within 48 hours. All deaths and significant changes were recorded [24].

Maintenance: Wild-type *Drosophila melanogaster* (Carolina Biological) were maintained at 19.1 ℃ in a 1:1.3 ratio of fly medium (Carolina Biological) to deionized H_2O, with 4-5 grains of yeast per vial. Newly enclosed flies were iced and sorted by sex. The males were aged in groups of 6-7 flies per vial. The food in the vials was changed once the food looked fully consumed and dead *D. melanogaster* were removed from vials to maintain food quality.

4 Results and Discussion

4.1 Computational Modeling and Ligand Selection

The objective of the computational phase was to design a novel CTSC inhibitor using 3,5-dimethoxycinnamic acid as a scaffold, with an improved docking score and ADME pharmacokinetic properties relative to CatC inhibitor 10 [14]. After the initial docking score screening, 26 compounds were selected for further pharmacokinetic, cytotoxicity, and Lipinski rule violation screening. As shown in **figure 10**, S228, achieved a docking score of -7.226, a 20.4% improvement over CatC inhibitor 10. S228 also achieved a QPlogHERG score of -5.734, 1 Lipinski rule violation, a QPlogS score of -1.346, a QPlogKhsa score of -0.696, and a CNS score of -2. All of these scores were within the optimal ranges for computational modeling and suggested that S228 would have a strong binding affinity to the Cathepsin C protein, while maintaining its favorable pharmacokinetic properties.

As shown in **figure 11**, S228 formed multiple stabilizing interactions within the CTSC binding site. Specifically, S228 formed 1 salt bridge and 2 hydrogen interactions with the critical CYS-234 residue, and 1 hydrogen bond with the ASN-380, ASP-1, NAG-1119, and THR-379 residues. Together, these interactions explain S228's high predicted docking score and its inhibitory potential. The combination of a high binding affinity, ideal pharmacokinetic properties, low cost, and synthetic feasibility, supported S228's selection for synthesis and in vivo testing.

Structure Name:	Docking Score:	QPlogHERG Score:	Lipinski's Rule of 5:	QPlogS Score:	QPlogKhsa Score:	CNS Score:
Ligand 1 (B22)	-5.998	-6.512	0	-3.361	-0.079	-2
Structure 105	-5.201	-4.345	0	-3.126	-0.284	-1
Structure 106	-5.899	-4.393	0	-2.751	-0.536	-2
Structure 110	-5.993	-5.087	0	-0.7	-0.586	-2
Structure 113	-5.821	-5.724	0	-0.972	-0.338	-1
Structure 114	-6.877	-4.743	1	-0.202	-0.722	-2
Structure 115	-5.996	-4.841	1	0.19	-0.871	-2
Structure 116	-6.953	-4.735	1	0.324	-0.969	-2
Structure 121	-6.571	-5.117	1	0.027	-0.895	-2
Structure 127	-6.591	-5.054	1	-0.181	-0.815	-2
Structure 128	-6.179	-4.733	1	0.526	-1.138	-2
Structure 129	-6.065	-4.837	1	0.436	-1.066	-2
Structure 137	-5.744	-3.822	0	-1.078	-0.807	-2
Structure 138	-5.717	-3.621	0	-1.458	-0.532	-2
Structure 151	-5.904	-4.626	0	-2.213	-0.74	-2
Structure 179	-5.917	-4.948	0	-2.213	-0.74	-2
Structure 181	-6.130	-5.757	0	-3.192	-0.569	-2
Structure 189	-6.903	-5.922	0	-4.123	-0.534	-2
Structure 194	-7.126	-5.948	0	-3.535	-0.803	-2
Structure 201	-6.420	-5.754	1	-0.638	-0.741	-2
Structure 206	-7.937	-5.736	1	-0.334	-0.928	-2
Structure 210	-5.620	-5.841	1	-0.476	-0.928	-2
Structure 211	-7.437	-5.889	1	-0.952	-0.745	-2
Structure 214	-6.735	-5.816	0	-0.998	-0.645	-2
Structure 227	-6.403	-5.672	0	-0.932	-0.69	-2
Structure 228	**-7.226**	**-5.734**	**1**	**-1.346**	**-0.696**	**-2**
Structure 229	-7.153	-5.693	1	-1.197	-0.715	-2
Very Good	-6.50<	-5.00<	1>	-1.5<	-1.5/1.5	-2
Decent	-6.49/-6.00	-5.99/-4.99	N/A	-1.99/-1.51	N/A	-1
Bad	-5.99>	-6.00>	2<	-2>	-1.5>/1.5<	0<

Figure 10: Computational Results for Top Candidates. Dark green scores indicate optimal values, light green scores indicate acceptable values, and red scores indicate values outside of the threshold, and were eliminated from contention. Structure 228 (S228) was selected for synthesis due to its synthesis feasibility, high docking score, and optimal ADME pharmacokinetic properties | Figure made by author using Google Sheets

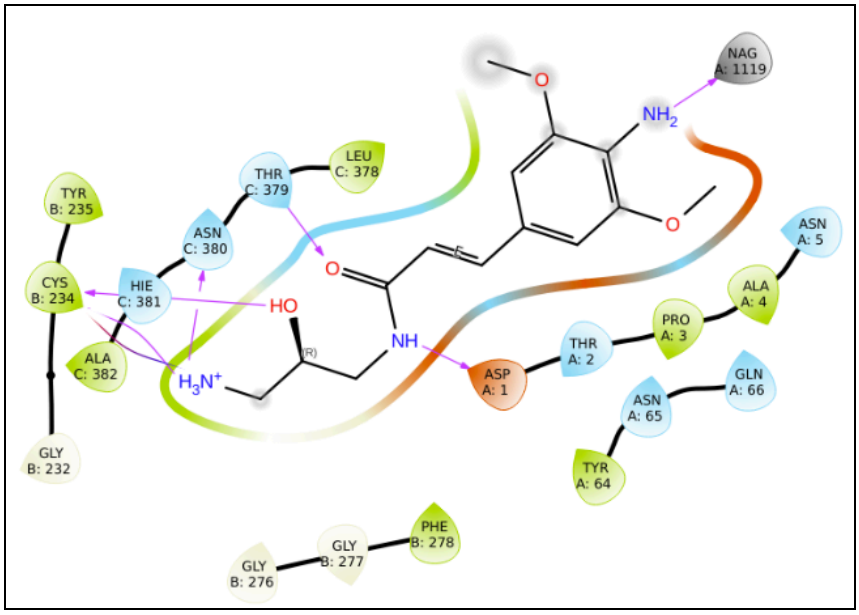

Figure 11: Ligand-protein interaction diagram of Structure 228 (S228) within the CTSC binding pocket. Pink arrows represent hydrogen bonds formed between S228 and key CTSC binding site residues, while Red/Blue arrows represent salt bridge interactions | Figure made by author using Schrödinger Maestro

4.2 Synthesis and Structural Verification

Step 1 Synthesis Verification: FTIR

A 3 step synthesis was developed to synthesize S228. The purpose of the step 1 reaction was to nitrate the dimethoxybenzene ring on position 4, which would allow nitro reduction to achieve the desired amine in a following step. Following the nitration reaction, an FTIR spectrum of compound 1 showed the appearance of two new distinct absorption peaks at about 1530 cm^{-1} and 1340 cm^{-1}, as shown in **figure 12,** that were absent in the overlaid FTIR spectrum of the starting molecule. The new peaks corresponded to the symmetric and asymmetric N=O bonds, key indicators of successful electrophilic aromatic nitration [25, 26, 27].

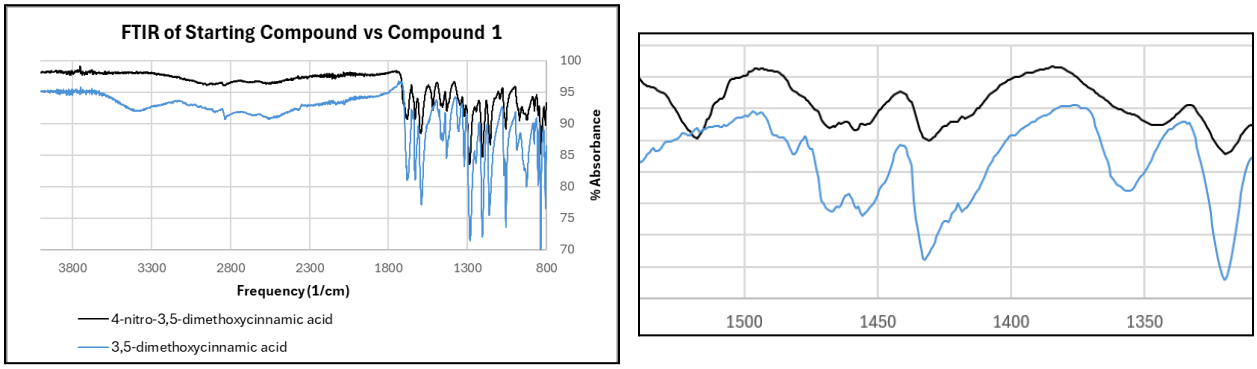

Figure 12: (Left) FTIR of starting molecule compared to compound 1, and (Right) Zoom on FTIR showing the appearance of N=O absorption peaks, at 1530 cm^{-1} and 1340 cm^{-1} | Figure made by author using Excel

Step 2 Synthesis Verification: FTIR

The purpose of the step 2 reaction was to link 1,3-diamino-2-propanol with 4-nitro-3,5-dimethoxycinnamic acid by turning the carboxylic acid into an amide. Following the conversion of the carboxylic acid to an amide, the FTIR spectrum of compound 2 showed clear changes consistent with successful amide conversion, when overlaid with an FTIR of compound 1. The strong C=O peak at about 1710 cm^{-1}, as shown in **figure 13**, disappeared in the products spectrum. In its place, a sharp amide C=O (amide 1) band appeared at about 1620-1640 cm^{-1} and a C-N (amide 2) stretch appeared at about 1445 cm^{-1}. Lastly, a broad band at about 3300 cm^{-1} appeared, corresponding to the overlapping N-H and O-H stretching bands from the amide and hydroxyl substituents [26, 27].

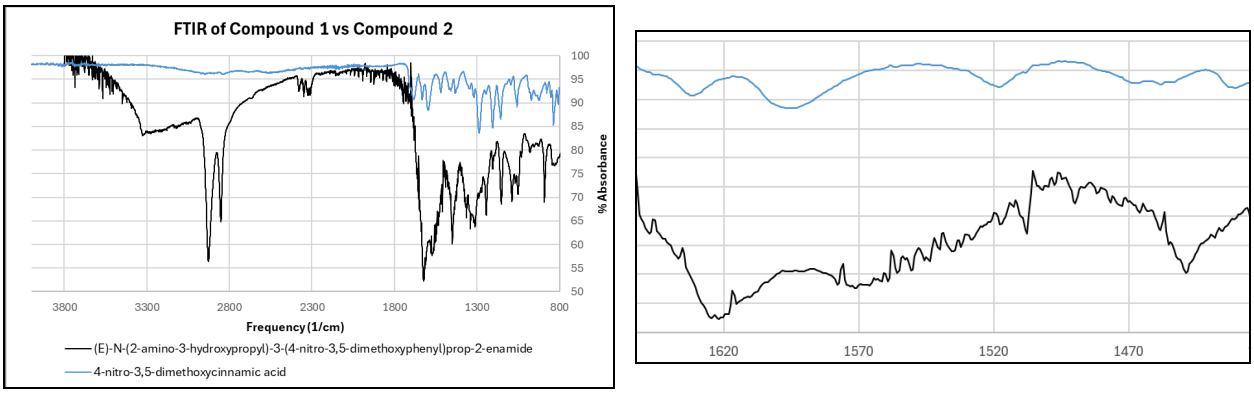

Figure 13: (Left) FTIR of compound 1 compared to compound 2, and (Right) Zoom on FTIR showing the appearance of C=O and C-N absorption peaks, at 1620 cm^{-1} and 1445 cm^{-1} respectively | Figure made by author using Excel

Step 3 Synthesis Verification: FTIR

The purpose of the step 3 reaction was to reduce the nitro group added in step 1 into an amine. Following the nitro reduction, the FTIR spectrum of S228 showed the disappearance of the asymmetric and symmetric N=O absorption peaks, at about 1530 cm^{-1} and 1340 cm^{-1}, as shown if **figure 14**, when overlaid with an FTIR of compound 2, indicating the reduction of the nitro functional group. Also, N-H stretching bands appeared at about 1620 cm^{-1} and 3300 cm^{-1}, confirming formation of the desired aromatic amine, and S228 [25, 26, 27].

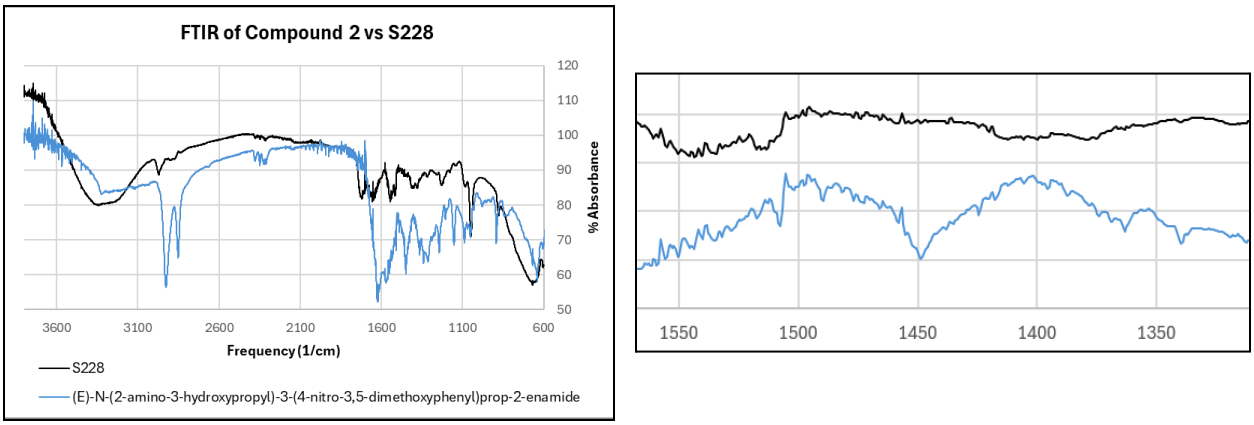

Figure 14: (Left) FTIR of compound 3 compared to S228, and (Right) Zoom on FTIR showing the disappearance of the N=O absorption peaks, at 1530 cm^{-1} and 1340 cm^{-1} | Figure made by author using Excel

Overall Synthesis Verification: ^{1}H-NMR

The purpose of conducting a ^{1}H-NMR spectroscopy on S228 was to further confirm successful synthesis of the final compound and verify its structure. S228's experimental ^{1}H-NMR spectra was compared to S228's predicted ^{1}H-NMR spectra in NMRium. The experimental spectrum showed two sharp singlets at 3.7-3.9 ppm, representing the two methoxy groups attached at the 3 and 5 positions of the benzene ring of

S228. There were also multiplets present in the 1.0-3.5 ppm range, corresponding to the aliphatic CH and CH_2 protons of the 1,3-diamino-2-propanol substituent. In the aromatic region, peaks appeared between 6.8-7.6 ppm, consistent with the expected aromatic protons of the benzene ring in S228. There were also multiplets present in the 4.5-5.0 ppm range, corresponding to the hydroxyl and amine group protons. The predicted and experimental spectra showed strong alignment in both the chemical shifts and relative intensities of the peaks, confirming that the synthesized compound structure matched with S228's structure. Overall, the ^{1}H-NMR data worked with the FTIR data, verifying the successful synthesis of S228.

4.3 Preventative Efficacy of S228: SMURF Assay

A characteristic structural change that occurs in IBD patients is a high gastrointestinal tract permeability, which can cause poor digestion, nutrient malabsorption, and a wide range of symptoms, as mentioned earlier. *Drosophila melanogaster* was identified as the optimal model organism for preliminary in vivo screening of the anti-inflammatory efficacy of S228 due to its physiological and genetic similarities with mammalian intestines, and semi-permeable intestinal anatomy. The objective of the SMURF assay was to visualize the integrity of the intestinal barrier in *D. melanogaster* when treated with various doses of S228. As shown in **figure 16**, the SMURF assay was used to test whether S228 could prevent intestinal barrier damage when given before DSS-induced IBD. After dissection and quantification of the average blue intestinal intensity using FIJI ImageJ, doses of 0.1 μM, 0.5 μM, and 2.5 μM of S228 yielded average blue intensities of 95.68%, 97.61%, and 98.40% respectively. The 0.1 μM and 2.5 μM doses of S228 reached p-values<0.05, while the 0.5 μM dose of S228 reached a p-value<0.01 when compared to the negative control w/IBD treatment group, which yielded an average blue intensity of 51.22%, as shown in **figure 16**. These statistical results suggest that S228 was very effective in preventing damage to the gut barrier and lowering intestinal permeability when given as a preventative treatment at all of the concentrations tested, even having higher average blue intensities than healthy *D. melanogaster*. But more specifically, these findings suggest that moderate concentrations of S228 are optimal for preventing intestinal barrier damage, while higher concentrations may cause mild stress responses in *D. melanogaster.*

Treatment:	Negative Control (5% Sucrose)	Negative Control w/ IBD (5% Sucrose and 4% DSS)	Preventative Group: 0.1 µM S228 w/ IBD (5% Sucrose and 4% DSS)	Preventative Group: 0.5 µM S228 w/ IBD (5% Sucrose and 4% DSS)	Preventative Group: 2.5 µM S228 w/ IBD (5% Sucrose and 4% DSS)	Therapuetic Group: 0.5 µM S228 w/ IBD (5% Sucrose and 4% DSS)
Trial 1	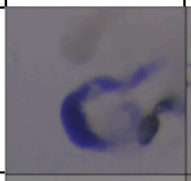	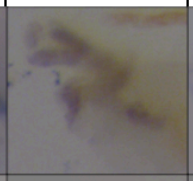	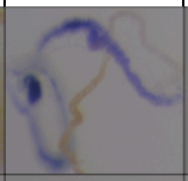	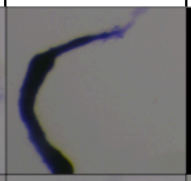	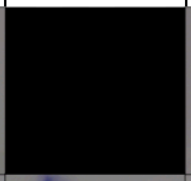	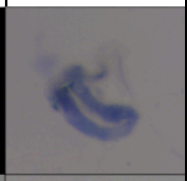
Trial 2	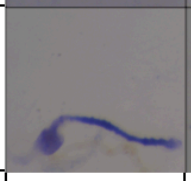	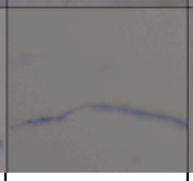	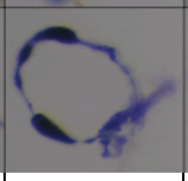	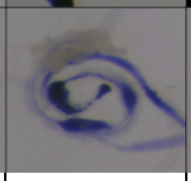	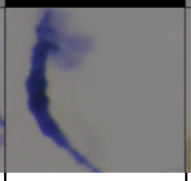	
Average Blue Intensity:	93.18%±10.11%	51.22%±7.78%	95.68%±2.83%	97.61%±5.76%	98.40%±1.44%	77.67%±3.61%

Figure 15: SMURF Assay Intestines Results. Flies were dissected and observed under a microscope. The blue dye intensity was quantified and the average percentage was calculated for each treatment group. A higher average blue intensity percentage indicates a healthier gut with less inflammation | Figure made by author using Google Slides

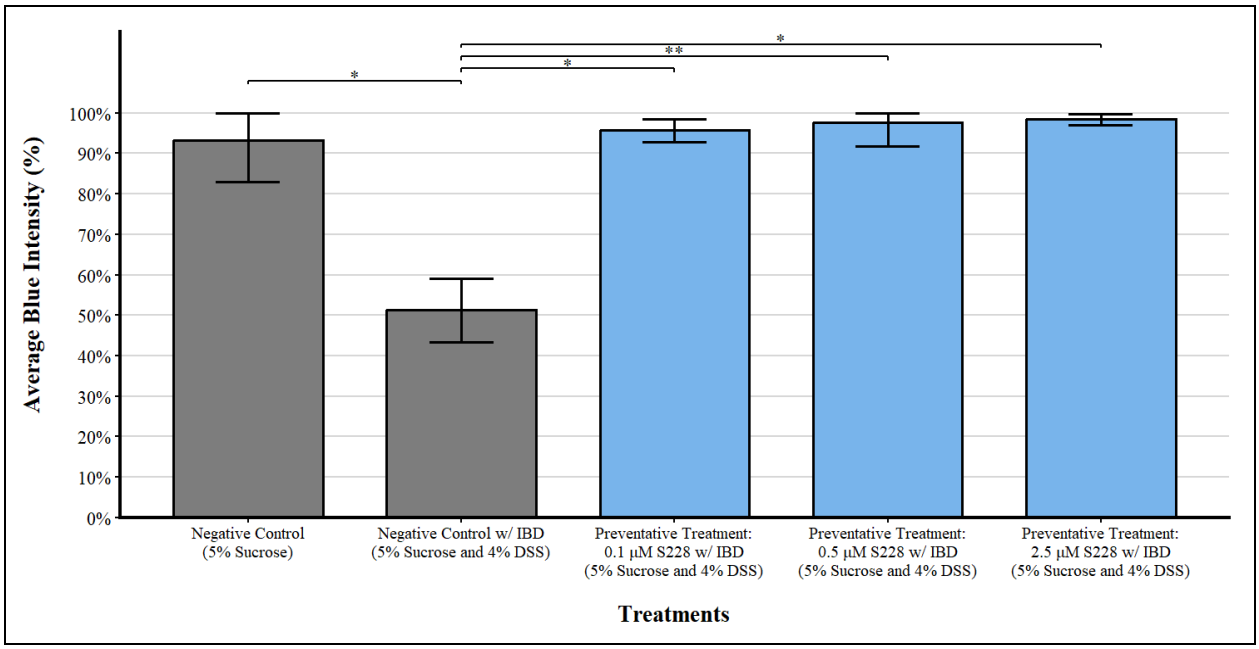

Figure 16: Average Blue Intensity for Preventative Treatment Comparison Graph. Flies were pre-treated with various dosages of S228 prior to DSS-induced IBD, to test S228 efficacy as a preventative treatment. Bars represent mean ± SD of blue intensity for each treatment group, with higher values indicating healthier, less inflamed intestines. A One-way ANOVA with Tukey's post-hoc test was conducted. Asterisks (*) denote significant differences relative to the negative control w/IBD group; *p<0.05, **p<0.01, and ns = not significant. Statistical analysis was conducted using RStudio software | Figure made by author using RStudio

4.4 Therapeutic Efficacy of S228: SMURF Assay

As shown in **figure 17**, the SMURF assay was also used to test whether S228 could limit intestinal barrier damage when given after DSS-induced IBD had already developed. Healthy flies on a control diet retained on average 93.18% blue intensity, while flies on a control diet with DSS-induced IBD retained on average 51.22% blue intensity, as shown in **figure 15**. Healthy flies that were treated with S228 after being exposed to DSS once again retained noticeable higher blue intensity on average. When given a dose of 0.5 µM of S228, a moderate recovery towards healthy levels was observed, retaining on average 77.67% blue intensity. Looking at **figure 15**, gut morphology appeared visually more intact under the microscope with the 0.5 µM dose, compared to the negative control with the IBD group. These results suggest the potential for S228 to restore the gut barrier integrity, even after inflammatory damage, having higher average blue intensities then *D. melanogaster* with IBD and no treatment. However, since statistical testing provided p-values>0.05, these findings suggest that S228 functions more efficiently as a preventative treatment than as a therapeutic treatment, although further experimentation is needed.

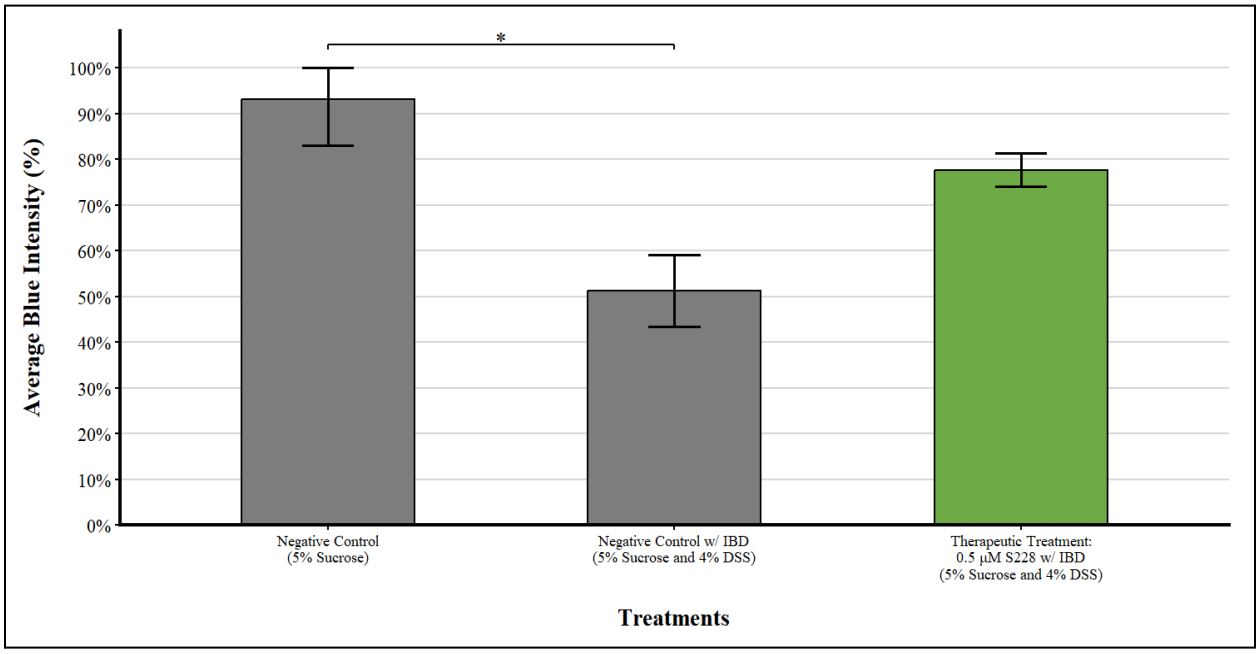

Figure 17: Average Blue Intensity for Therapeutic Treatment Comparison Graph. Flies were treated with various dosages of S228 after DSS-induced IBD, to test S228's efficacy as a therapeutic treatment. Bars represent mean ± SD of blue intensity for each treatment group, with higher values indicating healthier, less inflamed intestines. A One-way ANOVA with Tukey's post-hoc test was conducted. Asterisks (*) denote significant differences relative to the negative control w/IBD group; *p<0.05, **p<0.01, and ns = not significant. Statistical analysis was conducted using RStudio software | Figure made by author using RStudio

4.4 Toxicity Evaluation of S228: Survival Assay

The survival assay was used to test the lifespan of *D. melanogaster* with DSS-induced IBD in the presence of S228, and to determine S228's toxicity and protective effects when given as a preventative

and therapeutic treatment. Survival was recorded daily and analyzed using the Kaplan-Meier method with a log-rank (Mantel-Cox) test, which showed significant difference among treatment groups, with an overall p-value<0.0001, as shown in **figure 18**. In the preventative treatment groups, flies that received low to medium concentrations of S228, from 0.1 µM to 2.5 µM, had survival rates comparable to healthy control flies, suggesting these doses of S228 were not toxic and may have provided some protective benefit. However, at the highest concentration of S228, 5.0 µM, flies exhibited a rapid decline in survival, indicating dose-dependent toxicity.

In the therapeutic treatment groups, flies that received the lowest dose of S228, 0.1 µM, exhibited a rapid decline in survival, suggesting that a very low dose of S228 may not improve lifespan after DSS-induced IBD has developed, as shown in **figure 18**. Flies that received a medium-low dose of S228, 0.5 µM, had similar survival to DSS-induced IBD control flies, suggesting S228 did not significantly extend lifespan after DSS-induced IBD had developed. However, these flies did not show significant additional mortality, suggesting that S228 was well tolerated at a medium-low dose, even after IBD had developed. It is worth noting that some mortality may have been caused from flies sticking to the glass culture tubes they were maintained in rather than from physiological toxicity. Overall, these findings suggest that S228 is non-toxic at low to moderate doses and may even provide protective benefits when administered preventatively and when given therapeutically, only a medium low dose may extend survival, but will only moderately recover the gut barrier's integrity.

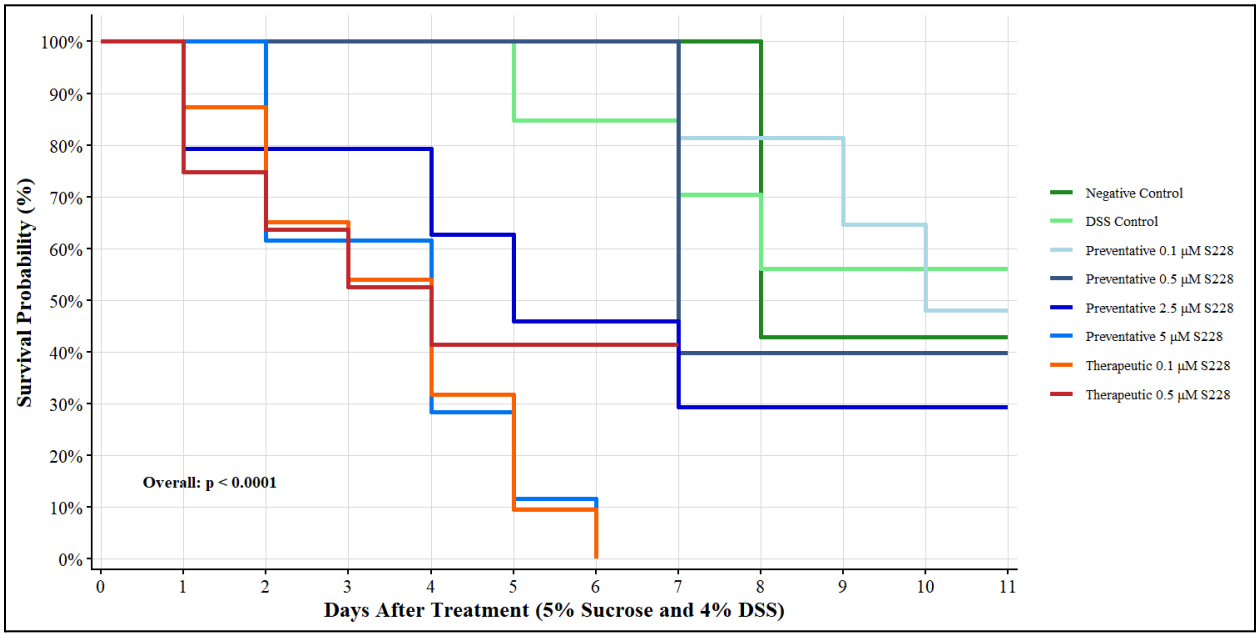

Figure 18: Survival curves for *D. melanogaster* treated with S228 under preventative and therapeutic treatments. Flies were treated with various dosages of S228 either before (preventative) or after (therapeutic) DSS-induced IBD, to evaluate S228's efficacy and potential toxicity. Survival probability (%) was calculated and analyzed using the Kaplan-Meier method with a log-rank (Mantel-Cox) test. The overall comparison across all

treatment groups was statistically significant ($p<0.0001$). Statistical analysis was conducted using RStudio software | Figure made by author using RStudio

5 Limitations

As always, there are some limitations to this research. Because *D. melanogaster* lacks a direct CTSC ortholog, these results cannot definitively confirm that S228 inhibits CTSC. The observed anti-inflammatory effects may be caused by alternate pathways and mechanisms. Due to the limited budget for this project, S228 couldn't be tested directly in a CTSC protein assay. Also, due to time and resource constraints on this project, experiments were conducted with small sample sizes, limiting the statistical power of the findings. A larger number ($n\geq30$) of *D. melanogaster* is needed to further validate and reproduce these conclusions. Other sources of variability may include fly handling during dissection, environmental factors that occurred during fly maintenance, and differences in lighting during image analysis. Therefore, all of these findings should be considered preliminary. Despite these limitations, the results provide promising early evidence that S228 is a low-toxicity inhibitor that has preventative and therapeutic benefits for IBD treatment.

6 Conclusion

This is the first known study that successfully designed, synthesized, and tested a 3,5-dimethoxycinnamic acid based small molecule inhibitor, S228, for Cathepsin C to treat IBD. Computational modeling identified S228 as a strong drug candidate due to its high docking score, favorable pharmacokinetic properties, and low synthesis cost. FTIR and ^{1}H-NMR spectroscopy confirmed S228's three step synthesis, expressing all of the expected peaks, and a purified product was achieved. In vivo results in *Drosophila melanogaster* demonstrated that S228 effectively preserved the intestinal barrier's integrity when under DSS-induced inflammatory conditions, and was well tolerated at low to moderate concentrations, showing S228's efficacy and safety in a biological organism.

These findings are significant because they show that modifying the 3,5-dimethoxycinnamic acid scaffold can yield a compound that has anti-inflammatory activity and good predicted CTSC binding activity for IBD treatment. This approach could provide a more effective and direct, cost-effective, and orally deliverable method for treating IBD, compared to traditional cytokine inhibitors. By combining computational design, chemical synthesis, and biological testing, this project created a framework for small-molecule drug discovery that is accessible, scalable, and is worthy of further development.

7 Future Directions

Future research will focus on conducting an in vitro cellular assay using purified human CTSC protein to validate S228's inhibitory activity. The optimization of the dose-dependent response of S228 will also be explored to find the most suitable dose for subsequent studies. To improve targeted biodelivery, the use of Cellulose acetate phthalate (CAP) will be further developed as a pH sensitive coating for S228. CAP dissolves at a pH of around 6.0, matching the environment of the duodenum, a primary location for inflammation in IBD. The goal of this coating would be to protect S228, shielding the drug from damage or degradation before it reaches the desired therapeutic region. Finally, S228 will be tested in mammalian models that directly possess a CTSC homolog comparable to a humans, to further validate S228's efficacy and toxicity in vivo.

8 Acknowledgments

I would like to thank my mentor, Dr. Timothy Anglin, and Dr. Michael Bruno for their constant support throughout this project, Dr. Heather Mallory, Mr. Antonio Lopez, and Dr. Darrell Spells, for their help with synthesis and biological testing, the NCSSM Summer Research and Innovation Program, the NCSSM Science Department, the NCSSM Foundation, for providing funding for this research, and my Research in Chemistry classmates, for helping make this research possible.

References

[1] CDC. “IBD Facts and Stats.” Inflammatory Bowel Disease (IBD), 22 July 2024, www.cdc.gov/inflammatory-bowel-disease/php/facts-stats/index.html.

[2] “Types of Inflammatory Bowel Disease.” Nyulangone.org, nyulangone.org/conditions/inflammatory-bowel-disease/types.

[3] Abegunde, Ayokunle T, et al. “Environmental Risk Factors for Inflammatory Bowel Diseases: Evidence Based Literature Review.” World Journal of Gastroenterology, vol. 22, no. 27, 2016, p. 6296, https://doi.org/10.3748/wjg.v22.i27.6296.

[4] Mayo Clinic. “Inflammatory Bowel Disease (IBD) - Diagnosis and Treatment - Mayo Clinic.” Mayoclinic.org, 2017, www.mayoclinic.org/diseases-conditions/inflammatory-bowel-disease/diagnosis-treatment/drc-20353320.

[5] Yang, Tao, et al. “Identification of a Novel 2,8-Diazaspiro[4.5]Decan-1-One Derivative as a Potent and Selective Dual TYK2/JAK1 Inhibitor for the Treatment of Inflammatory Bowel Disease.” Journal of Medicinal Chemistry, vol. 65, no. 4, 3 Feb. 2022, pp. 3151–3172, https://doi.org/10.1021/acs.jmedchem.1c01137.

[6] Strober, Warren, and Ivan J. Fuss. “Proinflammatory Cytokines in the Pathogenesis of Inflammatory Bowel Diseases.” Gastroenterology, vol. 140, no. 6, May 2011, pp. 1756–1767, https://doi.org/10.1053/j.gastro.2011.02.016.

[7] Abraham, Clara, et al. “Lessons Learned from Trials Targeting Cytokine Pathways in Patients with Inflammatory Bowel Diseases.” Gastroenterology, vol. 152, no. 2, 1 Jan. 2017, pp. 374-388.e4, https://doi.org/10.1053/j.gastro.2016.10.018.

[8] Zhao, Liang, et al. “Clinical Pharmacology Considerations in Biologics Development.” Acta Pharmacologica Sinica, vol. 33, no. 11, 1 Nov. 2012, pp. 1339–1347, https://doi.org/10.1038/aps.2012.51.

[9] Makurvet, Favour Danladi. “Biologics versus Small Molecules: Drug Costs and Patient Access.” Medicine in Drug Discovery, vol. 9, no. 9, Nov. 2020, p. 100075, https://doi.org/10.1016/j.medidd.2020.100075.

[10] Turk, Dušan, et al. “Structure of Human Dipeptidyl Peptidase I (Cathepsin C): Exclusion Domain Added to an Endopeptidase Framework Creates the Machine for Activation of Granular Serine Proteases.” The EMBO Journal, vol. 20, no. 23, 3 Dec. 2001, pp. 6570–6582, https://doi.org/10.1093/emboj/20.23.6570.

[11] Adkison, April M, et al. “Dipeptidyl Peptidase I Activates Neutrophil-Derived Serine Proteases and Regulates the Development of Acute Experimental Arthritis.” Journal of Clinical Investigation, vol. 109, no. 3, 1 Feb. 2002, pp. 363–371, https://doi.org/10.1172/jci13462.

[12] Aghdassi, Ali A., et al. “Cathepsin c Role in Inflammatory Gastroenterological, Renal, Rheumatic, and Pulmonary Disorders.” Biochimie, vol. 216, Jan. 2024, pp. 175–180, https://doi.org/10.1016/j.biochi.2023.09.018.

[13] Chitsamankhun, Chakriya, et al. “Cathepsin c in Health and Disease: From Structural Insights to Therapeutic Prospects.” Journal of Translational Medicine, vol. 22, no. 1, 20 Aug. 2024, https://doi.org/10.1186/s12967-024-05589-7.

[14] Chen, Xing, et al. “Identification of Novel Indolinone Derivatives as CTSC Inhibitors to Treat Inflammatory Bowel Disease by Modulating Inflammatory Factors.” European Journal of Medicinal Chemistry, vol. 280, 27 Sept. 2024, p. 116914, https://doi.org/10.1016/j.ejmech.2024.116914.

[15] Pagliari, Stefania, et al. “Antioxidant and Anti-Inflammatory Effect of Cinnamon (Cinnamomum Verum J. Presl) Bark Extract after in Vitro Digestion Simulation.” Foods, vol. 12, no. 3, 18 Jan. 2023, p. 452, https://doi.org/10.3390/foods12030452.

[16] Yeshi, Karma, et al. “Current Treatments, Emerging Therapeutics, and Natural Remedies for Inflammatory Bowel Disease.” Molecules, vol. 29, no. 16, 21 Aug. 2024, pp. 3954–3954, https://doi.org/10.3390/molecules29163954.

[17] Kikuzaki, Hiroe, et al. “Antioxidant Properties of Ferulic Acid and Its Related Compounds.” Journal of Agricultural and Food Chemistry, vol. 50, no. 7, 2002, pp. 2161–8, https://doi.org/10.1021/jf011348w.

[18] Schrödinger, LLC. “QikProp 4.4 User Manual.” Schrödinger, LLC. New York, NY, 2015.

[19] Calvo, Roxan, et al. “Facile Access to Nitroarenes and Nitroheteroarenes Using N-Nitrosaccharin.” Nature Communications, vol. 10, 30 July 2019, https://doi.org/10.1038/s41467-019-11419-y.

[20] Herrera-Guzmán, Karina, et al. “A Practical Method for the Synthesis of Small Peptides Using DCC and HOBt as Activators in H2O–THF While Avoiding the Use of Protecting Groups.” RSC Advances, vol. 14, no. 54, 1 Jan. 2024, pp. 39968–39976, https://doi.org/10.1039/d4ra07847k.

[21] Owsley, D. C., and Bloomfield, J. J. "The Reduction of Nitroarenes with Iron/Acetic Acid." Synthesis, no. 2, Feb. 1977, pp. 118-120, https://doi.org/10.1055/s-1977-24279.

[22] Capo, Florence, et al. “The Intestine of Drosophila Melanogaster: An Emerging Versatile Model System to Study Intestinal Epithelial Homeostasis and Host-Microbial Interactions in Humans.” Microorganisms, vol. 7, no. 9, 9 Sept. 2019, p. 336, https://doi.org/10.3390/microorganisms7090336.

[23] Martins, Raquel R., et al. “How to Catch a Smurf? – Ageing and Beyond… in Vivo Assessment of Intestinal Permeability in Multiple Model Organisms.” Bio-Protocol, vol. 8, no. 3, 5 Feb. 2018, https://doi.org/10.21769/BioProtoc.2722.

[24] Dan, Pallavi, et al. “Evaluation of Hydroxyapatite Nanoparticles - Induced in Vivo Toxicity in Drosophila Melanogaster.” Applied Surface Science, vol. 484, 1 Aug. 2019, pp. 568–577, https://doi.org/10.1016/j.apsusc.2019.04.120.

[25] “6.3: IR Spectrum and Characteristic Absorption Bands.” Chemistry LibreTexts, 15 Dec. 2021, chem.libretexts.org/Bookshelves/Organic_Chemistry/Organic_Chemistry_I_%28Liu%29/06%3A_Structural_Identification_of_Organic_Compounds-_IR_and_NMR_Spectroscopy/6.03%3A_IR_Spectrum_and_Characteristic_Absorption_Bands.

[26] Smith, Brian. “Organic Nitrogen Compounds, VII: Amides—the Rest of the Story.” Spectroscopy Online, 1 Jan. 2020, www.spectroscopyonline.com/view/organic-nitrogen-compounds-vii-amides-rest-story.

[27] LibreTexts Chemistry. “Infrared Spectroscopy Absorption Table.” Chemistry LibreTexts, 2014, chem.libretexts.org/Ancillary_Materials/Reference/Reference_Tables/Spectroscopic_Reference_Tables/Infrared_Spectroscopy_Absorption_Table.

[28] Livingston, Dawson B. H., et al. “Active Transport of Brilliant Blue FCF across the Drosophila Midgut and Malpighian Tubule Epithelia.” Comparative Biochemistry and Physiology Part A: Molecular & Integrative Physiology, vol. 239, 1 Jan. 2020, p. 110588, https://doi.org/10.1016/j.cbpa.2019.110588.